ENTHALPY-POROSITY TECHNIQUE FOR MODELING CONVECTION-DIFFUSION PHASE CHANGE: APPLICATION TO THE MELTING OF A PURE METAL

A. D. Brent , V. R. Voller & K. J. Reid

ENTHALPY-POROSITY TECHNIQUE FOR MODELING CONVECTION-DIFFUSION PHASE CHANGE: APPLICATION TO THE MELTING OF A PURE METAL

A. D. Brent, V. R. Voller, and K. J. Reid
Mineral Resources Research Center, University of Minnesota,
Minneapolis, Minnesota 55455

The melting of pure gallium in a rectangular cavity has been numerically investigated using the enthalpy-porosity approach for modeling combined convection-diffusion phase change. The major advantage of this technique is that it allows a fixed-grid solution of the coupled momentum and energy equations to be undertaken without resorting to variable transformations. In this work, a two-dimensional dynamic model is used and the influence of laminar natural-convection flow on the melting process is considered. Excellent agreement exists between the numerical predictions and experimental results available in the literature. The enthalpy-porosity approach has been found to converge rapidly, and is capable of producing accurate results for both the position and morphology of the melt front at different times with relatively modest computational requirements. These results may be taken to be a sound validation of this technique for modeling isothermal phase changes in metallurgical systems.

INTRODUCTION

Phase-change processes play an important role in both extraction and fabrication operations in the metallurgical industries. These processes involve complex heat and mass transfer phenomena that determine the ultimate strength and integrity of metallic components by governing the microstructures formed. The ability to predict phase-change phenomena in metallurgical systems is therefore of considerable engineering interest. A significant effort has recently been directed to the theoretical modeling of phase-change problems [1–12].

Phase change in a metallurgical system represents a moving-boundary problem. A number of techniques are available for the solution of these problems, and a comprehensive review can be found in Crank [1]. Much of the early work in this area was concerned primarily with phase change in which conduction was assumed to be the principal mechanism of energy transfer. In most practical situations involving a liquid/solid phase change, however, convection effects (either forced or free) are also of importance and in fact may totally dominate over conduction in some cases.

NOMENCLATURE

a	coefficients in the discretized energy equation	X	length of rectangular cavity
A	porosity function for the momentum equations	Y	height of rectangular cavity
d	source term in the discretized energy equation	α	thermal diffusivity, k/c
		β	volumetric coefficient of thermal expansion
c	specific heat	ΔH	nodal latent heat
C	morphology constant	ϵ	porosity of computational cell, $\Delta H/L$
f	latent heat function	λ	relaxation factor
g	acceleration due to gravity	μ	dynamic viscosity
h	sensible enthalpy	ρ	density
k	thermal conductivity		
L	latent heat of fusion	**Subscripts**	
Pr	Prandtl number, $c\mu/k$		
P	effective pressure	abs	quantity absorbed over a time step
Ra	Raleigh number, $g\beta(T_{hot} - T_{int})Y^3\rho^2/\alpha\mu$	error	error in conservation balance
S_b	buoyancy source term for v momentum equation	hot	heated wall conditions
		int	initial and cold wall conditions
S_h	source term for energy equation in terms of enthalpy	m	melting point
		n	iteration counter
S_T	source term for energy equation in terms of temperature	nb	neighboring node points
		p	pth node point or control volume
S_u	source term for u momentum equation	ref	reference conditions
S_v	source term for v momentum equation		
T	temperature		
u	velocity vector	**Superscript**	
u, v	velocity components in x and y directions	0	time-dependent coefficients, also old
x, y	coordinates		values at previous time step

The modeling methodologies developed for melting or solidification studies may broadly be classified into three groups:

1. *Empirical:* A possible engineering approach is to apply a conduction treatment and account for the enhanced energy transfer resulting from convection by boosting the liquid conductivity. This approach has been applied successfully to some metallurgical problems [13–15].

2. *Classical:* A more rigorous approach is to fully account for convection in the liquid region. This may involve deriving suitable governing heat and mass transfer equations and the development of accompanying numerical techniques for their solution. Difficulties arise if the governing equations are based on the classical Stefan formulation, i.e., a temperature-based heat transfer equation. The main reason for this is that in the vicinity of the phase change, conditions on temperature, velocity, and latent heat evolution have to be accounted for. This effectively rules out the application of a fixed-grid numerical solution, as deforming grids or transformed coordinate systems are required to account for the position of the phase front. Examples of combined convection/diffusion phase-change studies employing these techniques may be found in Sparrow et al. [2], Ramachandran et al. [3],

Gadgil and Gobin [4], Albert and O'Neill [5], and Sparrow and Ohkubo [6].

3. *Enthalpy:* An alternative to the empirical and classical approaches outlined above is the so-called enthalpy formulation, which allows a fixed-grid solution to be undertaken. This approach removes the need to explicitly satisfy conditions at the phase front and is therefore able to utilize standard solution procedures for the fluid flow and energy equations directly, without re-sorting to mathematical manipulations and transformations. This approach is particularly attractive in cases where phase change may constitute only part of a complex problem. Examples of fixed-grid solutions of convective/ diffusion phase-change problems may be found in Morgan [7], Gartling [8], and Voller et al. [9–12].

The enthalpy methods account for the latent heat in the energy equation by assigning a nodal latent heat value to each computational cell according to the tem-perature of the cell. Upon changing phase, the nodal latent heat content of the cell is adjusted to account for latent heat absorption or evolution, this adjustment being reflected in the energy equation as either a heat source or sink. A distinctive ad-vantage of this arrangement is that no explicit conditions for energy conservation at the solid/liquid interface need to be accounted for. A major problem, however, with fixed-grid solution procdures, is accommodating the zero velocity condition, which is required as a liquid region turns to solid. Various methods have been used to "switch off" velocities in computational cells that are freezing (or "switch on" ve-locities in the case of melting). Velocities may simply be set to zero in a compu-tational cell when the mean latent heat content reaches some predetermined value between 0 (cell all solid) and L (cell all liquid), where L is the latent heat of the phase change [7]. A somewhat more subtle approach is employed by Gartling [8], in which the viscosity of a cell is driven to a very large value as the latent heat content of the cell falls to zero. This increasing viscosity provides the necessary coupling between the physical state of the material in the cell and the momentum equations, thereby driving velocities to zero in cells that are solid. Voller et al. [9–12] have examined various methods for dealing with the zero solid velocity condition in fixed-grid solutions for freezing in a thermal cavity, and have proposed an alter-native but similar approach to that adopted by Gartling. Computational cells that are undergoing a phase change (i.e., $0 < \Delta H < L$) are modeled as pseudo-porous media, with the porosity, ϵ, being a function of ΔH and ranging between 1 (fully liquid cell) and 0 (fully solid cell). The present work involves the application of this "en-thalpy-porosity" technique to the two-dimensional melting of a pure metal in a rect-angular cavity. A comparison is made between the results predicted by this method and experimental values available in the literature in order to validate the applica-bility of this technique for metal systems.

THE ENTHALPY–POROSITY APPROACH

In considering the phase change of an alloy, three distinct regions will be pres-ent: a solid region, a totally liquid region, and a mushy region consisting of liquid

dispersed among solid dendrites. To model such a phase change, the basic conservation equations have to be solved throughout the calculation domain.

Governing Equations

The energy equation may be written in terms of the sensible enthalpy, $h = \int_{T_{ref}}^{T} c \, dT$ as follows [12]:

$$\frac{\partial(\rho h)}{\partial t} + \text{div}(\rho \mathbf{u} h) = \text{div}(\alpha \text{ grad } h) + S_h \tag{1}$$

where α is the thermal diffusivity (k/c), and S_h is a source term that will be discussed in more detail below. In the full liquid and mushy regions, fluid flow equations are required. These equations consist of the conservation of momentum equations (one for each velocity component) and a conservation of mass equation. Under the assumptions of Newtonian laminar flow, these equations are

$$\frac{\partial(\rho u)}{\partial t} + \text{div}(\rho \mathbf{u} u) = \text{div}(\mu \text{ grad } u) - \frac{\partial P}{\partial x} + Au \tag{2}$$

$$\frac{\partial(\rho v)}{\partial t} + \text{div}(\rho \mathbf{u} v) = \text{div}(\mu \text{ grad } v) - \frac{\partial P}{\partial y} + Av + S_b \tag{3}$$

$$\frac{\partial \rho}{\partial t} + \text{div}(\rho \mathbf{u}) = 0 \tag{4}$$

where $\mathbf{u} = (u,v)$ is the velocity, P is an effective pressure, and μ is the viscosity. Assuming the Boussinesq treatment to be valid—i.e., density is constant in all terms except a gravity source term—natural-convection effects can be accounted for on defining the buoyancy source term to be

$$S_b = \frac{\rho_{ref} g \beta (h - h_{ref})}{c} \tag{5}$$

where β is a thermal expansion coefficient and h_{ref} and ρ_{ref} are reference values of enthalpy and density, respectively. The function of the parameter A in the momentum equations will be discussed more fully below.

Source Terms

In using a fixed-grid approach for the analysis of solidification and melting systems, a central difficulty is in accounting for mass and heat transfer conditions in the vicinity of the phase change. The basic approach for overcoming this problem is to define appropriate volume source terms for the governing equations. In the enthalpy-porosity approach, the latent heat evolution is accounted for on defining the energy-equation source term [S_h in Eq. (1)] to have the form [12]:

$$S_h = \frac{\partial(\rho\ \Delta H)}{\partial t} + \mathrm{div}(\rho\mathbf{u}\ \Delta H) \tag{6}$$

where $\Delta H = f(T)$, the latent heat content, is defined as a function of temperature. In the case of an isothermal phase change, the term $\mathrm{div}(\rho\mathbf{u}\ \Delta H)$ vanishes and the function $f(T)$ will be defined as follows:

$$f(T) = \begin{array}{ll} L & T > T_m \\ 0 & T < T_m \end{array} \tag{7}$$

where T_m is the phase-change temperature and L is the latent heat of fusion. For a mushy-region phase change, the temperature and latent heat relationship can be found via experiment or one of the available metallurgical relationships; e.g., the Scheil equation [16] can be used.

The condition that all velocities in solid regions are zero is accounted for in the enthalpy-porosity approach by appropriately defining the parameter A in Eqs. (2) and (3). The basic principle is gradually to reduce the velocities from a finite value in the liquid, to zero in the full solid, over the computational cells that are changing phase. This can be achieved by assuming that such cells behave as porous media with porosity ϵ = the "element liquid fraction" [12]. The porosity can be computed as $\Delta H/L$ (i.e., the fraction of liquid in the cell), where ΔH is the latent heat content of the cell in question. In cells that are undergoing a phase change, A is defined so that the momentum equations are forced to mimic Carman-Kozeny equations for flow in a porous media [12]:

$$\mathrm{grad}\ P = \left[-C\frac{(1 - \epsilon)^2}{\epsilon^3} \right]\mathbf{u}_a \tag{8}$$

where C is a constant accounting for the mushy-region morphology and $\mathbf{u}_a$ is an apparent velocity. In order to achieve this behavior, an appropriate definition of A is

$$A = -C\frac{(1 - \epsilon)^2}{\epsilon^3 + b} \tag{9}$$

where b is merely a computational constant introduced to avoid division by zero.

In practice the effect of A is as follows: In full liquid elements, A is zero and has no influence; in elements that are changing phase, the value of A will dominate over the transient, convective, and diffusive components of the momentum equations, thereby forcing them to imitate the Carman-Kozeny law; in totally solid elements, the final large value of A will swamp out all terms in the governing equations and force any velocity predictions effectively to zero. The validity of the Carman-Kozeny equation in describing the flow in a dendritic mushy region has been investigated experimentally [17], and thus application of Eq. (9) has physical significance. Further details on the implementation of the enthalpy-porosity approach for

mushy-region phase changes can be found in [9–12]. It should be noted that the constant C may significantly influence the morphology of the phase front, and care must be taken in assigning a value to it. This constant effectively controls the degree of penetration of the convection field into the mushy region. Further work needs to be carried out in the area of mushy-region phase change to establish guiding principles in assigning appropriate values for both the constants C and b in Eq. (9).

In the case of an isothermal phase change, however, the flow inside computational cells that are melting or freezing does not follow the governing laws for flow in a porous media. In an isothermal phase-change system, the phase front is a well-defined line and has no band or width associated with it as in the case of a mushy phase change. In a discretized calculation domain, however, the phase front will have a finite width associated with it. This width will generally be only that of a single computational cell, and hence any convenient method for gradually extinguishing the velocities in a solidifying cell will be acceptable. A possible alternative to applying the Carman-Kozeny equations is to use a linear function for A, that is,

$$A = -C(1 - \epsilon) \qquad (10)$$

One advantage of using a simple linear function is that it is slightly less expensive to compute than the Carman-Kozeny formula. The influence of A will again be gradually to override the other terms in the discretized momentum equations in solidifying control volumes, thereby forcing velocity predictions in solid regions to zero. Although the value of the constant C in Eqs. (9) and (10) will not influence the morphology of the phase front as significantly as in the case of a mushy-region phase change, it should be sufficiently large to force velocity predictions in solid regions essentially to zero. It should be mentioned that although any convenient method may be acceptable for extinguishing velocities in solidifying cells in isothermal phase-change systems, it is desirable that the method chosen allows a smooth, gradual transition rather than a step change in velocity. Step changes in the momentum-equation source terms tend to retard convergence of their numerical solution, and sometimes lead to oscillations that may result in divergence. Inappropriate switching methods for the velocities may also lead to reduced accuracy, particularly when coarse grids are employed. A quantitative evaluation of the influence of different switching techniques has been conducted by Voller et al. [10].

Numerical Implementation of the Enthalpy-Porosity Technique

Once a suitable expression has been selected for the velocity-switching function A in the momentum equations, standard solution procedures for the coupled momentum and continuity equations may be used without any modification. In this study, the SIMPLE procedure described by Patankar was applied [18]. To ensure a converged solution of the energy equation, however, special treatment of the enthalpy source term [Eq. (6)] is required. In the numerical solution of the energy equation, the latent heat content of each control volume needs to be updated according to the temperature values predicted from the energy equation after each iteration in the computational cycle. A reliable method for updating the latent heat content of each computational cell has been developed by Voller et al. [10, 12]. This

method avoids oscillations in the iterative procedure that could result in the inability to achieve a converged solution, and may be applied in both finite-element- and control volume-based finite-difference numerical schemes. As a control volume-based numerical scheme was used in this work, the following discussion will be limited to the control volume approach. Following the control volume-based formulation and notation in Patankar [18], the discretized energy equation [Eq. (1)] may be written as follows:

$$a_p h_p = \Sigma a_{nb} h_{nb} + a_p^0 h_p^0 + d \tag{11}$$

where the subscripts indicate the appropriate node point values, the a's are coefficients that depend on the combined convection/diffusion fluxes into the pth control volume, d contains energy sources and sinks for the pth control volume, and a_p^0 is the unsteady coefficient linking the present h_p value to its value at the previous time step, h_p^0. For this discretized energy equation, the nodal latent heat value for the pth control volume is updated after the nth iteration according to Voller et al. [10, 12] as

$$[\Delta H_p]_{n+1} = [\Delta H]_n + \frac{a_p}{a_p^0}\{[h_p]_n - c \cdot f^{-1}[\Delta H_p]_n\} \tag{12}$$

where f^{-1} is the inverse of the latent heat function [Eq. (7) for an isothermal phase change] used to describe the latent heat content of each computational cell. The enthalpy update expression given by Eq. (12) is entirely general, i.e., it is applicable to both mushy-region phase changes that occur over a temperature range as well as to isothermal phase changes. It is only the form of the latent heat function $f(T)$ that would distinguish an isothermal phase change from a phase change occurring over a temperature range. As this work is concerned with the application of the enthalpy-porosity technique to a pure metal system, the following discussion will be restricted to isothermal phase changes. It should be noted that during iterations it is possible that use of Eq. (12) to update the nodal latent heat values may lead to nonphysical values, i.e., nodal latent heat values greater than L or less than zero. The first of these conditions will occur if more than an entire control volume changes phase in a single time step, and the second may arise if a control volume is close to starting the phase change at the beginning of a time step. To prevent the nodal latent heat contents from assuming physically unrealistic values, the iterative update of $[\Delta H_p]_{n+1}$ should be restricted between zero and L. For an isothermal phase change, the computational implementation of the enthalpy update given by Eq. (12) may thus be simply accomplished as follows:

$$[\Delta H_p]_{n+1} = [\Delta H]_n + \frac{a_p}{a_p^0} \cdot c \cdot \lambda \cdot \{[T_p]_n - T_m\}$$

$$\text{set } [\Delta H_p]_{n+1} = 0 \text{ if } [\Delta H_p]_{n+1} < 0 \tag{13}$$

$$\text{set } [\Delta H_p]_{n+1} = L \text{ if } [\Delta H_p]_{n+1} > L$$

where λ is a relaxation factor.

Equation (13) illustrates the physical significance of the enthalpy update, i.e., the nodal latent heat values are adjusted according to the difference between the nodal temperature predicted from the energy equation and the phase-change temperature. In the case of freezing, the nodal latent heat value assigned to computational cells undergoing a phase change provides a heat source in the energy equation to account for latent heat evolution. This source expires when the latent heat content of the cell is exhausted. At this point $\Delta H_p = 0$ and the cell is totally solid. Conversely, in a melting situation the nodal latent heat value of a computational cell undergoing a phase change provides the energy equation with a heat sink to account for the absorption of latent heat. This sink disappears when the total latent heat of the phase change is reached. At this point $\Delta H_p = L$ and the cell is totally fluid. While iterating, corrections in the nodal latent heat values of computational cells in which a phase change is occurring are driven by the difference between the temperature predicted from the energy equation and the phase-change temperature. The enthalpy update scheme attempts to annihilate this difference so that at convergence, the temperature of all cells in which both liquid and solid coexist will be that of the phase-change temperature, T_m. This scheme thus accurately reflects the physical state of an isothermal phase change in a discretized domain, i.e., the phase front is "smeared" across the width of the computational cells in which the phase change is occurring.

The ratio a_p/a_p^0 in the nodal latent heat update arises from the derivation of Eq. (12) [12] and is a "normalizing" factor that accounts for the number of grid points and size of time step used. This ratio increases upon both grid refinement and on increasing size of time step, thereby compensating for these changes in the enthalpy update equation and ensuring rapid convergence of the method. The physical significance of the a_p/a_p^0 term is as follows:

1. For a given size of time step, a larger number of control volumes will change phase during any particular time step if a fine grid is used. As the a_p/a_p^0 term increases as a function of the number of grid points, it forces more rapid changes in the nodal enthalpy values near the phase front when a fine grid is employed. This allows the true position of the phase front to be quickly established in the discretized domain.

2. For a fixed grid size, increasing the size of the time step results in a larger number of control volumes changing phase during each time step. As the value of the ratio a_p/a_p^0 increases according to the time step size, this term ensures rapid changes in the nodal enthalpy values in the region of the phase change when large time steps are used. This again quickly establishes the true position of the phase front in the discretized domain.

MELTING OF PURE GALLIUM IN A RECTANGULAR CAVITY

To verify the applicability of the enthalpy-porosity approach to metallurgical systems, the modeling of an isothermal phase change was undertaken for which reliable experimental data exists in the literature. The study examined the two-dimensional melting of pure gallium in a rectangular cavity with one heated wall. This subject was chosen for the following reasons.

1. If the enthalpy-porosity technique is to be applied to metallurgical systems, it is essential to verify the accuracy of its predictions for a substance that is representative of metal properties. Comparisons to other materials such as water/ice or organic phase-change materials (PCMs) may not be valid if the technique is to be used for metallurgical applications. Large dissimilarities between the thermophysical properties of organic compounds and metals result in considerably different flow structures and phase-front morphologies [19–21].

2. Gallium has a melting point close to the ambient (29.78°C), and experiments with it may therefore be well controlled and are able to yield complete information about a melting or freezing front (e.g., the shape and position of the front may be traced at different times). The high melting temperatures of most practical structural metals (e.g., steel and titanium) are not conducive to experimentation, and great difficulties exist with obtaining reliable phase-change data for these materials. As a result of the convenience of working with gallium, experimental data available in the literature may be assumed to be both comprehensive and accurate.

3. A comprehensive experimental study on the melting of gallium in a rectangular cavity has been conducted by Gau and Viskanta [21]. The authors present detailed traces of the morphology of the melt front at various times. The narrow temperature range (10°C) used by these investigators allows the assumption of constant physical properties, which simplifies a computational simulation of this work. The results obtained by Gau and Viskanta [21] also show a great deal of morphology of the melt front. It is believed that if the numerical analysis is capable of accurately predicting the acute morphology obtained in the experiments, this would represent a sound validation of the enthalpy-porosity approach for isothermal phase changes in metallurgical systems.

It should be noted that there is no fundamental difference between applying the enthalpy-porosity technique to either melting or solidifcation problems. The equations and numerical scheme developed for melting are equally applicable to freezing situations; the particular type of phase change that occurs is determined only by the initial and boundary conditions of the problem.

Calculation Domain

A diagram of the calculation domain and boundary conditions is given in Fig. 1. The values of T_{int}, T_{hot}, X, and Y were taken from one of Gau and Viskanta's experiments [21] for which the melt front had been traced in detail at a number of different times. With reference to Fig. 1, these values were $T_{int} = 28.3°C$, $T_{hot} = 38°C$, $X = 8.89$ cm, and $Y = 6.35$ cm. The physical properties for pure gallium are well documented [22–25], and the values used in this investigation are given in Table 1. The physical property values were chosen at 32°C, a temperature that is representative of the temperature range of the experiment (i.e., 28.3–38°C). The Prandtl number for liquid gallium at this temperature is 0.0216, and the situation shown in Fig. 1 corresponds to a Stefan number of 0.039 and a Raleigh number of 6×10^5.
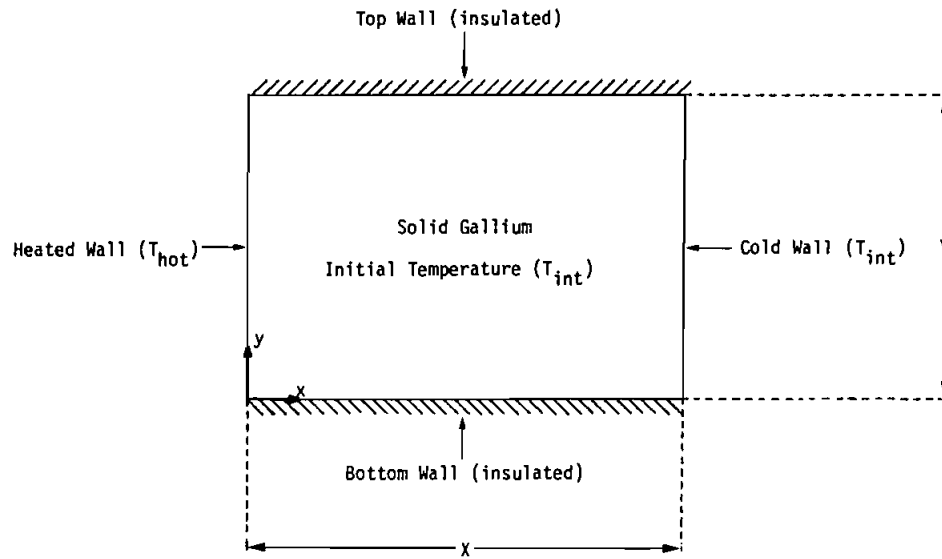
Fig. 1   Calculation domain and boundary conditions.

It should be mentioned at this point that while gallium may be an ideal metal for phase-change studies from an experimental point of view, the fact that the thermal conductivity of solid, crystalline gallium is highly anisotropic complicates a theoretical analysis. The conductivity of the solid crystal ranges from 88.5 $W \cdot m^{-1} \cdot K^{-1}$ along the b axis to 16 $W \cdot m^{-1} \cdot K^{-1}$ along the c axis [22]. The thermal conductivity of polycrystalline gallium at the melting point (29.78°C) is 33.5 $W \cdot m^{-1} \cdot K^{-1}$ [22]. However, the problem of anisotropic solid thermal conductivity is alleviated to a large degree by examining a melting rather than a feezing problem. In melting, the only disturbance the system is subjected to when the experiment is started at time t = 0, is that one of the walls is heated to a temperature above the melting pint (see Fig. 1). Once melting is initiated against this wall, all the heat transfer into the system occurs through a layer of molten liquid. It is therefore the physical properties of the liquid rather than the solid that will govern the phase change in a melting process. If freezing is studied, however, the major resistance to energy transport resides in a solid layer growing on a cold wall, and it is then the thermal conductivity

Table 1   Physical Properties of Pure Gallium

Density (liquid), ρ	6093 $kg \cdot m^{-3}$
Reference density, ρ_{ref}	6095 $kg \cdot m^{-3}$
Reference temperature, T_{ref}	29.78°C
Volumetric thermal expansion coefficient of liquid, β	1.2×10^{-4}
Thermal conductivity, k	32.0 $W \cdot m^{-1} \cdot K^{-1}$
Melting point, T_m	29.78°C
Latent heat of fusion, L	80160 $J \cdot kg^{-1}$
Specific heat capacity, C	381.5 $J \cdot kg^{-1}$
Dynamic viscosity, μ	1.81×10^{-3} $kg \cdot m^{-1} \cdot s^{-1}$
Prandtl number, Pr	2.16×10^{-2}

of the solid that exerts a controlling influence on the phase change. The problems associated with freezing studies on gallium have been noted by Gau and Viskanta [21], who were unable to obtain reproducible results for the phase front position and morphology when conducting solidfcation studies on the metal. It should be noted that although the thermal conductivity of liquid gallium is also anisotropic (although to a lesser degree than that of the solid) [22], the presence of convection currents will tend to average out directional differences in thermal conductivity.

Numerical Solution

The conservation equations assuming two-dimensional laminar flow in cartesian coordinates with constant physical properties are given in the appendix, along with appropriate boundary conditions for this problem. These equations represent a set of four nonlinear, coupled partial differential equations, which were solved iteratively using the control volume-based finite-difference procedure described by Patankar [18]. A fully implicit formulation was used for the time-dependent terms and the combined convection/diffusion coefficients were evaluated using Patankar's power law scheme. The SIMPLE algorithm was applied to solve the momentum and continuity equations to obtain the velocity field. A line-by-line solver based on the TDMA was used to iteratively solve the algebraic discretization equations. Details of the numerical method and solution procedures may be found in Patankar [18]. The nodal enthalpy update procedure described by Voller et al. [10, 12] was used to iteratively adjust nodal enthalpy values [i.e., Eq. (13)]. A flow chart of the computational algorithm is given in Fig. 2.

After conducting a grid-refinement study, a uniform 42×32 grid was chosen for this work. A time step of 5 s was applied for the first four time steps to resolve the rapid initial changes in temperature near the heated wall, after which a constant time step of 10 s was used. Further refinements in the grid or time step size did not produce discernable improvements in accuracy. In order to be consistent with the general methodology developed for mushy-region phase changes, the Carman-Kozeny formula [Eq. (9)] was applied for switching the velocities in cells undergoing a phase change. A value of 1.6×10^6 was used for the morphology constant C and a value of 1×10^{-3} for the constant b in Eq. (9). Underrelaxation factors of 0.5, 0.6, and 0.9 were used for the solution of the two momentum equations, the pressure correction equation, and the energy equation, respectively. Underrelaxation of the enthalpy update [Eq. (13)] was also required to avoid divergence in this highly nonlinear, coupled situation. It was found advantageous to ramp the underrelaxation factor λ in Eq. (13) from an initial value of 0.2 at the beginning of each time step to a maximum of 0.4 as convergence was neared. The position of the phase front at desired times was determined by plotting the $L/2$ nodal latent heat contour. This was found to provide a smoother, more precise estimate of the phase-front position than a plot of the melting-point isotherm. The reason for this is that all control volumes in which both liquid and solid coexist will be at the melting point (T_m), and hence the T_m isotherm represents a band rather than a well-defined line. The rationale behind using the $L/2$ contour is the assumption that the phase front at any given time passes through control volumes that posses half the latent heat of the phase change.
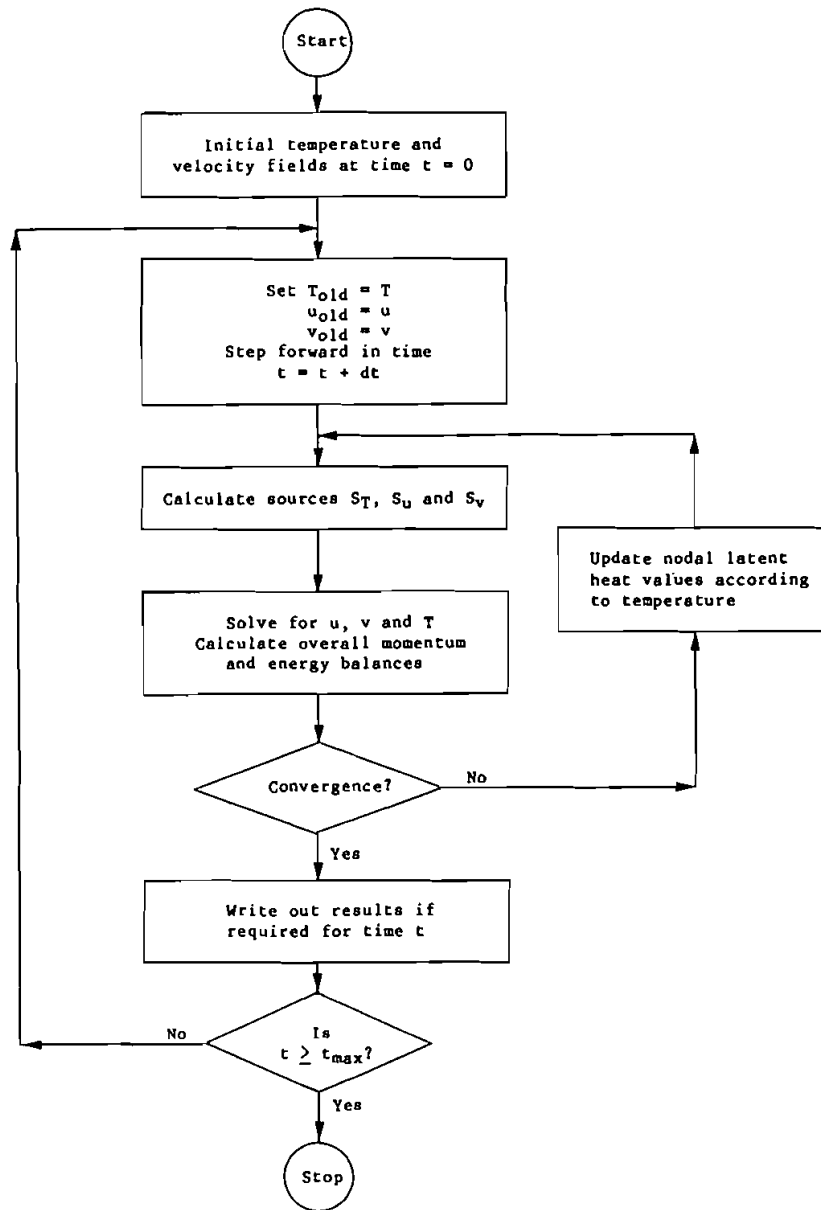
Start

Initial temperature and
velocity fields at time t = 0

Set T_{old} = T
u_{old} = u
v_{old} = v
Step forward in time
t = t + dt

Calculate sources S_T, S_u and S_v

Update nodal latent
heat values according
to temperature

Solve for u, v and T
Calculate overall momentum
and energy balances

Convergence?   No

Yes

Write out results if
required for time t

No   Is
t $\geq$ t_{max}?

Yes

Stop

Fig. 2 Flow chart of the computational algorithm.

Convergence Criteria and Computational Requirements

The convergence criteria for the numerical solution of the conservation equations given in the appendix were based on both the maximum local mass imbalance within the cavity (reflecting convergence of the flow field) and on an unsteady overall energy balance (indicating convergence of the energy equation). As the energy equation contains a source term (viz., the latent heat term $\rho(\partial \Delta H/\partial t)$] that is not coupled directly to the momentum equations, it is necessary to monitor both the mass

and energy balances to ensure a fully converged solution. The unsteady energy balance was calculated as the sum of the total energy flowing into the cavity at the two end walls and the energy absorbed by the material in the cavity, over each time step Δt, as follows:

$$Q_{error} = Q_{x=0} + Q_{x=X} + Q_{abs} \tag{14}$$

where

$$Q_{x=0} = \Delta t \int_0^Y k \frac{dT}{dx}\bigg|_{x=0} dy \tag{15}$$

$$Q_{x=L} = -\Delta t \int_0^Y k \frac{dT}{dx}\bigg|_{x=L} dy \tag{16}$$

and

$$Q_{abs} = \rho \int_0^Y \int_0^X [c(T - T_{old}) + (\Delta H - \Delta H_{old})] \, dx \, dy \tag{17}$$

The energy absorption term contains a contribution from the latent heat change over the time step. The integrals in Eqs. (15)–(17) were evaluated numerically by summing over the respective control volumes. The temperature derivatives in Eqs. (15) and (16) were evaluated in a fully implicit manner to be consistent with the numerical scheme used. Convergence was declared after the maximum local mass imbalance became less than $1 \times 10^{-4}\%$ of the total mass present in the cavity and the absolute value of the energy balance error dropped below $1 \times 10^{-2}\%$. Increasing the stringency of the convergence criteria beyond these values did not result in significant improvements in accuracy. An average of 43 iterations per time step were needed to achieve convergence. The computations were conducted on both an AT&T 3B2/400 microcomputer and a Cray 2/1 supercomputer. The longest simulation carried out (i.e., a melt time of 19 min, spanning 116 time steps) required 26 CPU hours on the microcomputer and 9 CPU min on the supercomputer. No attempt was made to optimize or vectorize the code. Such steps may be expected to produce significant reductions in CPU times. In particular, code vectorization would result in substantially faster execution on the Cray 2/1. However, these CPU times compare very favorably with those quoted in the literature for comparable investigations [26, 27]. These requirements may still be considered modest for the complex problem investigated, and indicate that two-dimensional fine-grid solutions based on the enthalpy-porosity technique are entirely feasible using a microcomputer. For three-dimensional phase-change analyses, however, it is anticipated the application of vectorized code on a supercomputer would be required to yield acceptable execution times.

Results and Discussion

The position of the melt front and streamlines at 3, 6, 10, and 19 min are shown in Figs. 3a–6a. The melt front is virtually planar after 3 min as the natural
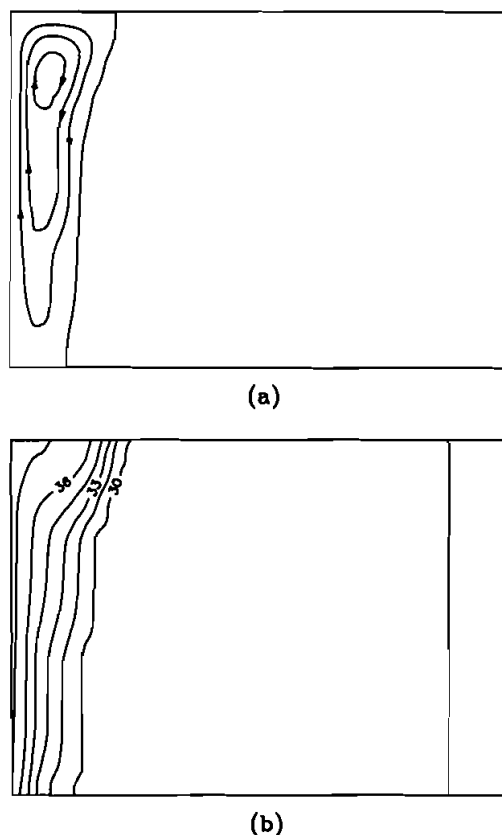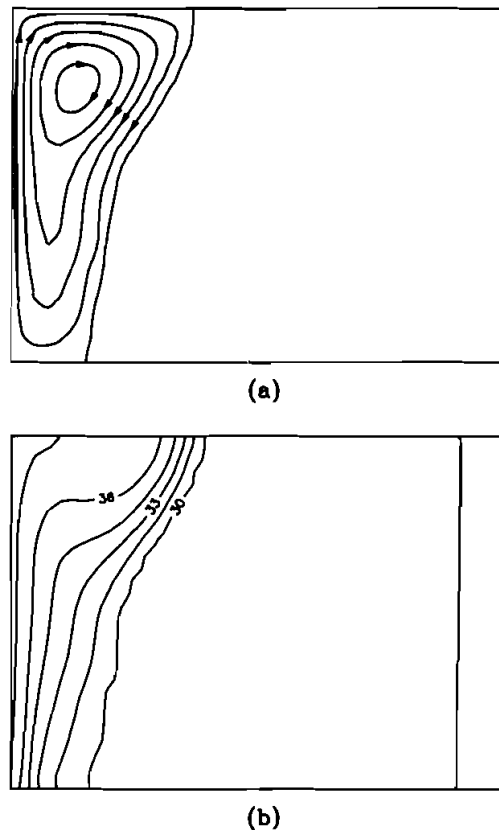
(a)

(b)

Fig. 3   Flow and temperature fields at 3 min for the
two-dimensional melting of gallium. Panel (a) depicts
the streamlines and melt front; panel (b) the isotherms.

convection field has just begun to develop (Fig. 3a). Figure 4a shows the developing morphology after 6 min when the natural convection has intensified and is beginning to have a pronounced influence on the overall energy transport from the heated wall to the melt face. The morphology of the melt front is as expected; fluid rising at the heated wall travels across the cavity and impinges on the upper section of the solid front, thereby resulting in this area melting back beyond the mean position of the front. The influence of the convection currents intensifies with time, and the morphology of the melt front becomes more acute as melting progresses. Figures 5a and 6a show the melt front and streamlines after 10 and 19 min, respectively. From Fig. 6a it is evident that after 19 min the shape of the melt front is governed primarily by convection effects, with conduction exerting very little influence. Although the upper section of the melt front advances rapidly due to the impingement of warm fluid, the lower section moves considerably slower, thereby resulting in the acute morphology illustrated in Fig. 6a.Development of the intensity of the free convection field may be traced by examining Fig. 7, in which the maximum absolute value of the stream function is plotted against time. In the early stages of melting the max-

imum absolute value of the stream function increases rapidly as the temperature gradients driving the convection currents begin to develop. As the volume of the molten fraction in the cavity increases with time, the influence of viscous stresses against the cavity walls decrease, thereby allowing the fluid velocity (and consequently the absolute value of the stream function) to rise. The fluid motion continues to intensify until it levels off after approximately 12 min, by which time the natural convection field in the cavity is well developed.

The regions of maximum heat flux may be identified by examining the isotherm plots given in Figs. 3b–6b. The steepest temperature gradients are present in two areas, viz., at the upper section of the melt face where warm fluid impinges on the solid, and at the lower section of the heated wall where cool fluid returning from the melt front impinges on the heated wall. The "insulating" nature of the melt front in the cavity is also evident from the isotherm plots. Almost the entire temperature drop across the cavity occurs in the molten region, leaving the temperature of the residual solid essentially uniform near the initial temperature. The reason for this is that virtually all the energy entering the cavity at the heated wall is absorbed by the

(a)

(b)

Fig. 4   Flow and temperature fields at 6 min for the two-dimensional melting of gallium. Panel (a) depicts the streamlines and melt front; panel (b) the isotherms.
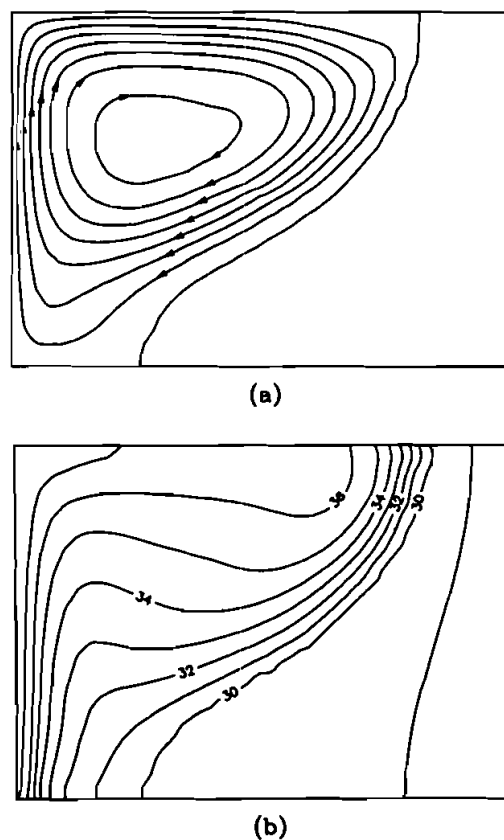
(a)

(b)
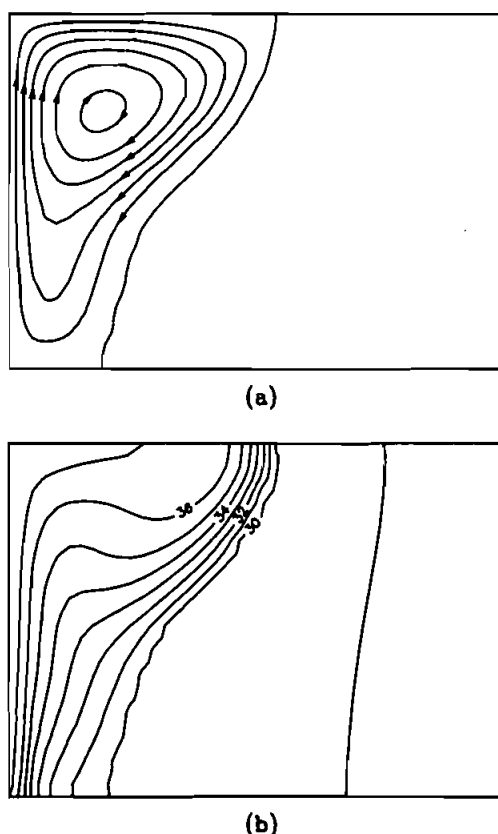
Fig. 5 Flow and temperature fields at 10 min for the two-dimensional melting of gallium. Panel (a) depicts the streamlines and melt front; panel (b) the isotherms.

phase change at the melt front, allowing only a small fraction to penetrate the slightly supercooled solid. As the major temperature gradients occur in the liquid phase, it is the thermal conductivity of the liquid rather than the solid that controls heat transfer, and hence the problems associated with the theoretical treatment of anisotropic solid conductivity do not arise.

The melt fronts calculated in this study and those determined experimentally by Gau and Viskanta [21] at various times are plotted in Fig. 8. From Fig. 8 it is evident that both the qualitative behavior and acute morphology of the experimental melt fronts have been realistically duplicated in the numerical study. An appreciation of the accuracy of the numerical predictions may be obtained by studying Fig. 9, in which the computed fronts at 2, 6, 10, and 17 min are compared directly to their experimental counterparts. Excellent agreement exists between the computed and experimental melt front positions, and small discrepancies between the measured and calculated results may be attributed to factors such as three-dimensional effects in the experimental apparatus used to determine the front position, experimental error, and variations in fluid properties.

(a)

(b)

Fig. 6 Flow and temperature fields at 19 min for the two-dimensional melting of gallium. Panel (a) depicts the streamlines and melt front; panel (b) the isotherms.
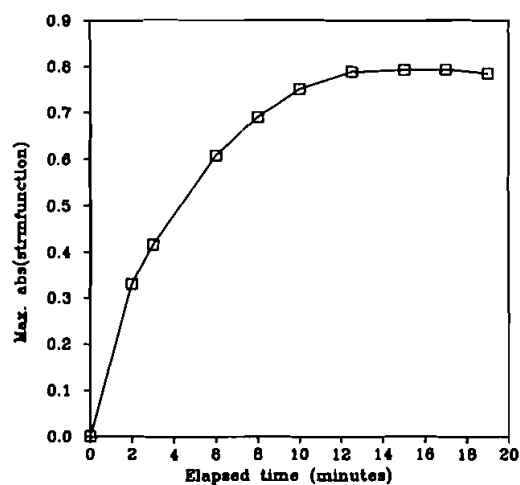

Fig. 7 Relationship between the maximum absolute value of the stream function and time for the two-dimensional melting of gallium.

313

CONCLUSIONS

The applicability of the enthalpy-porosity technique for modeling an isothermal phase change in a metallurgical system has been verified by examining the two-dimensional melting of pure gallium under the influence of natural convection in a rectangular cavity. Results obtained from this numerical study were compared to experimental data available in the literature. The method converges rapidly and is capable of accurately predicting both the position and morphology of the melt front at various times with relatively modest computational requirements. The results of this work may be taken to be a sound validation of the enthalpy-porosity technique for simulating isothermal phase changes in metallurgical systems.
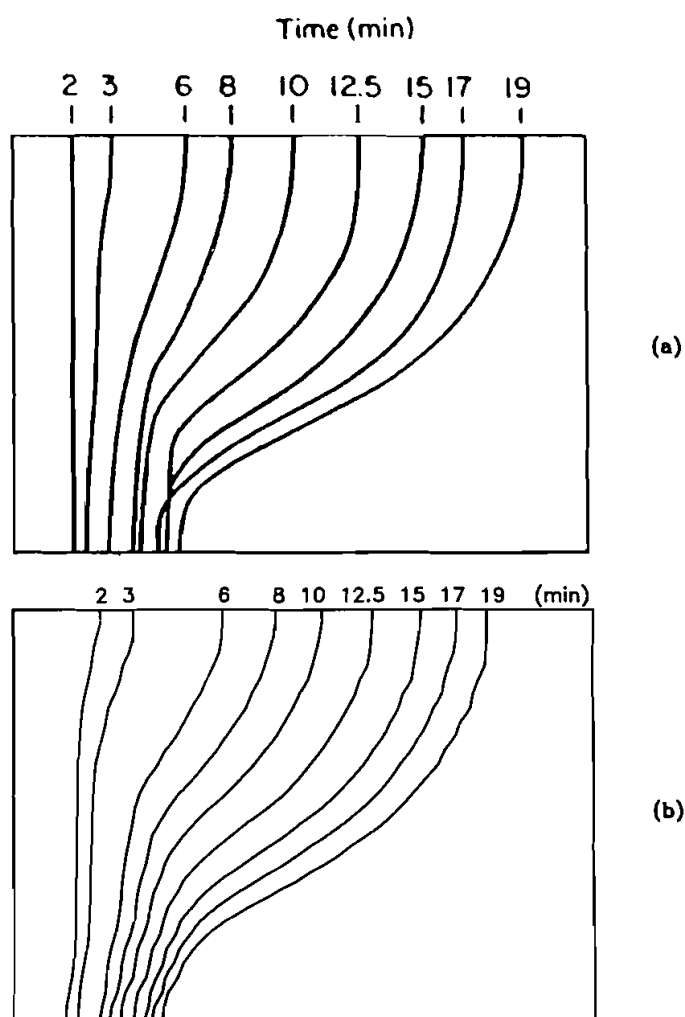
Fig. 8 Calculated and experimental melt fronts at various times. Panel (a) shows melt front positions determined experimentally by Gau and Viskanta [21]; panel (b) depicts the theoretical melt front positions calculated in this study.

— — — Numerical
— — — Experimental (Gau and Viskanta [21])
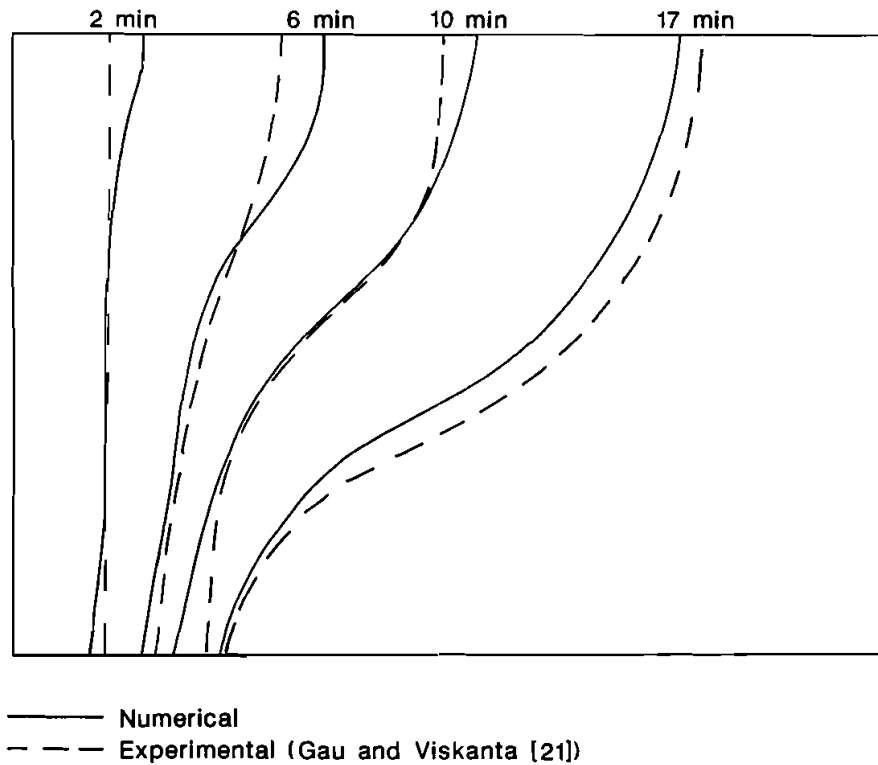
Fig. 9   Comparison of calculated and experimental melt fronts for the two-dimensional melting of gallium.

Validation of this approach for mushy phase-change systems is to be considered next. A detailed study of the quantitative influence of the morphology constant C in a mushy phase-change situation is also required as the criteria for assigning a value to this parameter need to be established. The application of the enthalpy-porosity method to the modeling of "freeze-linings" or "skulls" in metallurgical processes will also be undertaken. The ability to predict both the morphology and position of these protective solid layers that isolate a melt from the structural components of the vessel in which it is contained is of particular interest in the field of ultra-pure metals processing.

APPENDIX

Conservation Equations and Boundary Conditions for the Two-Dimensional Melting of Gallium

1. Conservation equations
   1.1 Continuity

$$\frac{\partial u}{\partial x} + \frac{\partial v}{\partial y} = 0$$

1.2 Momentum equations

x direction:

$$\rho\left(\frac{\partial u}{\partial t} + u\frac{\partial u}{\partial x} + v\frac{\partial u}{\partial y}\right) = \mu\left(\frac{\partial^2 u}{\partial x^2} + \frac{\partial^2 u}{\partial y^2}\right) - \frac{\partial P}{\partial x} + S_u$$

y direction:

$$\rho\left(\frac{\partial v}{\partial t} + u\frac{\partial v}{\partial x} + v\frac{\partial v}{\partial y}\right) = \mu\left(\frac{\partial^2 v}{\partial x^2} + \frac{\partial^2 v}{\partial y^2}\right) - \frac{\partial P}{\partial y} + S_v$$

where

$$S_u = Au$$

$$S_v = Av + \rho_{ref}g\beta(T - T_{ref})$$

1.3 Energy equation

$$\rho c\left(\frac{\partial T}{\partial t} + u\frac{\partial T}{\partial x} + v\frac{\partial T}{\partial y}\right) = k\left(\frac{\partial^2 T}{\partial x^2} + \frac{\partial^2 T}{\partial y^2}\right) + S_T$$

where

$$S_T = \rho\frac{\partial\Delta H}{\partial t}$$

2. Boundary conditions

2.1 Left wall ($x = 0$):

$$u = v = 0$$

$$T = T_{hot}$$

2.2 Top and bottom walls ($y = 0$ and $y = Y$):

$$u = v = 0$$

$$\frac{\partial T}{\partial y} = 0$$

2.3 Right wall ($x = X$):

$$u = v = 0$$

$$T = T_{cold}$$

REFERENCES

1. J. Crank, *Free and Moving Boundary Problems,* Clarendon Press, Oxford, 1984.
2. E. M. Sparrow, S. V. Patankar, and S. Ramadhyani, Analysis of Melting in the Presence of Natural Convection in the Melt Region, *J. Heat Transfer,* vol. 99, pp. 520–526, 1977.
3. N. Ramachandran, J. R. Gupta, and T. Jalunu, Thermal and Fluid Flow Effects During Solidification in a Rectangular Cavity, *Int. J. Heat Mass Transfer,* vol. 25, pp. 187–194, 1982.
4. A. Gadgil and D. Gobin, Analysis of Two-Dimensional Melting in Rectangular Enclosures in the Presence of Convection, *J. Heat Transfer,* vol. 106, pp. 20–26, 1984.
5. M. R. Albert and K. O'Neill, Transient Two-Dimensional Phase Change with Convection Using Deforming Finite Elements, in R. W. Lewis et al. (eds), *Computer Techniques in Heat Transfer,* vol. 1, Pineridge Press, Swansea, 1985.
6. E. M. Sparrow and Y. Ohkubo, Numerical Analysis of Two-Dimensional Transient Freezing Including Solid-Phase and Tube-Wall Conduction and Liquid-Phase Natural Convection, *Numer. Heat Transfer,* vol. 9, pp. 59–77, 1986.
7. K. Morgan, A Numerical Analysis of Freezing and Melting with Convection, *Comp. Methods Appl. Eng.,* vol. 28, pp. 275–284, 1981.
8. D. K. Gartling, Finite Element Analysis of Convective Heat Transfer Problems with Phase Change, in K. Morgan et al. (eds.), *Computer Methods in Fluids,* Pentech, London, 1980.
9. V. R. Voller, N. C. Markatos, and M. Cross, Solidification in Convection and Diffusion, in N. C. Markatos et al. (eds.), *Numerical Simulations of Fluid Flow and Heat/Mass Transfer Processes,* Springer-Verlag, Berlin, 1986.
10. V. R. Voller, N. C. Markatos, and M. Cross, Techniques for Accounting for the Moving Interface in Convection/Diffusion Phase Change, in R. W. Lewis and K. Morgan (eds.), *Numerical Methods in Thermal Problems,* vol. 4, Pineridge Press, Swansea, 1985.
11. V. R. Voller, M. Cross, and N. C. Markatos, An Enthalpy Method for Convection/Diffusion Phase Change, *Int. J. Numer. Methods Eng.,* vol. 24, pp. 271–284, 1987.
12. V. R. Voller and C. Prakash, A Fixed Grid Numerical Modelling Methodology for Convection/Diffusion Mushy Region Phase Change Problems, *Int. J. Heat Mass Transfer,* vol. 30, pp. 1709–1719, 1987.
13. C. Gau and R. Viskanta, Melting and Solidifcation of a Metal System in a Rectangular Cavity, *Int. J. Heat Mass Transfer,* vol. 27, pp. 113–123, 1984.
14. J. Szekely and P. S. Chhabra, The Effects of Natural Convection on the Shape and Movement of the Melt-Solid Interface in the Controlled Solidification, *Met. Trans. B,* vol. 1, pp. 1195–1203, 1970.
15. F. M. Chiesa and R. I. L. Guthrie, Natural Convection Heat Transfer Rate During the Solidification and Melting of Metals and Alloy Systems, *J. Heat Transfer,* vol. 99, pp. 520–526, 1977.
16. W. Kurz and D. J. Fisher, *Fundamentals of Solidifcation,* Trans. Tech., Switzerland, 1986.
17. D. R. Poirier, Permeability for Flow of Interdendritic Liquid in Columnar-Dendritic Alloys, *Met. Trans. B.,* vol. 18B, pp. 245–256, 1987.
18. S. V. Patankar, *Numerical Heat Transfer and Fluid Flow,* Hemisphere, Washington, D.C., 1980.
19. C. Benard, D. Gobin, and F. Martinez, Melting in Rectangular Enclosures: Experiments and Numerical Simulations, *J. Heat Transfer,* vol. 107, pp. 794–802, 1985.
20. B. W. Webb and R. Viskanta, Natural-Convection-Dominated Melting Heat Transfer in an Inclined Rectangular Enclosure, *Int. J. Heat Mass Transfer,* vol. 29(2), pp. 183–192, 1986.

21. C. Gau and R. Viskanta, Melting and Solidification of a Pure Metal on a Vertical Wall, *J. Heat Transfer*, vol. 108, pp. 174–181, 1986.

22. W. H. Cubberley (ed.), *Metals Handbook—Properties and Selection: Nonferrous Alloys and Pure Metals*, 9th ed., American Society of Metals, Metals Park, Ohio, pp. 736–737, 1979.

23. Gallium and Gallium Compounds, in *Kirk-Othmer Encyclopedia of Chemical Technology*, 3d ed., vol. 11, p. 606, Wiley, New York.

24. M. J. Duggin, The Thermal Conductivity of Liquid Gallium, *Phys. Lett.*, vol. 29A(8), pp. 470–471, 1969.

25. A. O. Ukanwa, Diffusion in Liquid Metal Systems, NASA Contractor Technical Report NASA-CR-144016, p. 9, June 1975.

26. C. J. Ho and R. Viskanta, Heat Transfer During Melting from an Isothermal Vertical Wall, *J. Heat Transfer*, vol. 106(c), pp. 12–19, 1984.

27. G. E. Schneider, Computation of Heat Transfer with Solid/Liquid Phase Change Including Free Convection, *J. Thermophys. Heat Transfer*, vol. 1(2), pp. 136–145, 1987.

Requests for reprints should be sent to V. R. Voller.